Astron. Astrophys. 363, 995–1004 (2000)

ASTRONOMY AND ASTROPHYSICS

Spectral variability of luminous early type stars

I. Peculiar supergiant HD199478

N. Markova and T. Valchev

Institute of Astronomy and Isaac Newton Institute of Chile Bulgarian Branch, National Astronomical Observatory, P.O. Box 136, 4700 Smoljan, Bulgaria (rozhen@mbox.digsys.bg)

Received 15 June 2000 / Accepted 8 September 2000

Abstract. We have obtained time-series of high-quality $H\alpha$ spectra with high resolution in wavelength (R = $\lambda/\delta\lambda$ of 15000 to 22000) and time (Δt =1d) of the late-type B supergiant HD199478. The spectra were analysed in terms of line-profile variability (lpv) using contemporary techniques of time-series analysis, such as Temporal Variance Spectrum and the 2d- Discrete Fourier Transform. The $H\alpha$ profile is found to consist of a highly variable emission core (between -280 and +150 km s^{-1}) superimposed on almost constant, extended ($\pm$1000 km s^{-1}) emission wings. Due to the lack of strong line-emission, the latter is attributed to electron-scattering in deep atmospheric layers.

The $H\alpha$ variability manifests itself by variations in velocity and intensity of blue- and red-shifted emission peaks, which result in drastic alterations in the shape of the profile from almost symmetric and unshifted emission, with respect to the stellar rest frame, through blue- or red-shifted asymmetric emission, to double-peaked emission or a reverse P Cygni-type profile. Significant variations in total emissivity (i.e. EW) of the line are also noted, but these variations do not appear to be obviously linked to changes in the line-profile shape. The pattern of variability resembles that in Be-stars - though on a much shorter time scale - and suggests interpretation in terms of an axially symmetric and perturbed stellar wind. Since the time-scale of the V/R variations is found to be 3 to 5 times longer than the radial fundamental pulsation period but consistent with rotational period, rotational modulation as a possible cause for this variability is considered.

Besides variations in $H\alpha$, continuous changes in velocity (typical dispersion of $\sigma \sim 5$ km s^{-1}) and strength, i.e. EW, (up to 13% of the mean) of a sample of three absorption lines ($CII\lambda\lambda 6583$, 6578 and $HeI\lambda 6678$) were also observed. The phenomenon observed is more likely connected to changes in velocity and temperature structures of the stellar photosphere. Pulsation instability as a possible cause of photospheric variability is suggested.

Key words: line: profiles – stars: early-type – stars: emission-line, Be – stars: individual: HD 199478

Send offprint requests to: N. Markova

1. Introduction

High-resolution, time-resolved IAU spectral observations showed that winds of luminous OB stars are highly variable on time-scales of hours to days and months. The most remarkable signs of this variability are Discrete Absorption Components, which migrate from red to blue throughout unsaturated P Cygni profiles of UV resonance lines. Coordinated UV and Hα spectroscopy suggests that structures responsible for DAC-related variability more likely originate close to or at the stellar surface (Kaper et al. 1997). On the other hand, modern studies of line-profile variability (lpv) have convincingly shown that photospheric variability is very common among early type stars (Baade 1992; Fullerton et al. 1996). The coexistence of photospheric and wind variability and the rough similarity of their time-scales implies that the two phenomena might be linked in some way.

In recent years, many efforts have been directed towards finding observational evidence for a direct coupling between processes going on in the stellar photosphere and in the wind (the so-called "photospheric connection"). The task, however, turned out to be difficult since it requires long sets of high-quality, time-resolved, wide-spectral window observations (note that lines formed in different regions of the star, i.e. in the wind and in the photosphere, must be traced simultaneously). Parallel photometric observations are also extremely useful since they provide direct evidence for variations in the stellar parameters. For these reasons the results reported in the literature, though promising, are far from convincing. At present, the star ζ Pup (O4 I(n)f) appears to be the best candidate to demonstrate the "photospheric connection" in the case of OB supergiants (Reid & Howarth 1996), although this assertion is disputable (Kaper et al. 1997). While the hypothesis of "photospheric connection" has not been discussed in relation to wind variability of LBVs, it is also worth noting the works of Markova (2000) and Markova et al. (2000) on P Cygni. Based on direct comparison of UBV photometry and optical spectroscopy the authors found a clear correlation between variations in the V-band and changes in the velocity of the absorption trough of a variety of lines formed in different wind layers, which they interpreted as possible evidence for a dynamic response of the stellar wind to small variations in basic parameters.

HD 199478 is a supergiant of spectral class B8Iae, which appears as a central star of the reflection nebula IC 5076. Its parameters are listed in Table 1. The star is distinguished from other B supergiants in that it shows spectral characteristics (e.g. inverse Balmer progression (Denizman & Hack 1988) and a double-peaked $H\alpha$ emission (Rosendhal 1973)), that suggest a definite similarity to Be stars. Variations in velocity of Balmer and metal lines were established by Denizman & Hack (1988). However, since the results originate from snapshot observations, neither typical time-scales nor behaviour pattern of the variability was stated. Observations in the UV reveal the presence of blue-shifted absorption components (Bates, Halliwell, Brown-Kerr 1986). The time-behaviour of the DACs is unknown. HD199478 is found to be a photometric variable. Small variations (amplitude of about 0.1 mag) in V- and B-bands were reported by Percy et al. (1988, 1997). The properties of this micro-variability have not been specified yet.

The purpose of our work is to investigate the spectral behaviour of HD199478 in order to establish different kinds of line-profile variability (lpv), to specify their properties, and to search for possible relationships between them. Simultaneously studying lines formed in different regions of the star (i.e. in the wind and in the photosphere), we hope to gain a better understanding of the nature and origin of variability in this object. The observational material and its reduction are described in Sect. 2. In Sect. 3 the temporal behaviour of Hα, $HeI\lambda6678$ and the CII resonance doublet is examined using contemporary techniques of time-series analysis, such as Temporal Variance Spectrum (TVS) and two dimensional Discrete Fourier Transform (2d-DFT). Some line-parameters such as radial velocity and equivalent width are measured and analysed in terms of time-variability.

Table 1. Stellar parameters of HD199478

Parameters	Value	References
V	5.69^m	Lennon et al. (1992)
$B-V$	$+0.46^m$	Lennon et al. (1992)
$E(B-V)$	0.47	Lennon et al. (1992)
$r[kps]$	1.84	Denizman & Hack (1988)
$\log T_{eff}$	4.097	McErlean et al. (1999)
$\log L/L_\odot$	4.89	McErlean et al. (1999)
$\log R/R_\odot$	1.92	Leitherer (1988)
$\log M/M_\odot$	1.17	Leitherer (1988)
$\log g$	1.56	McErlean et al. (1999)
$V_{sys}\sin i$ [km s^{-1}]	-16	Denizman & Hack (1988)
$V_{rot}\sin i$ [km s^{-1}]	45	McErlean et al. (1999)
$V_{\inf}$ [km s^{-1}]	400	Leitherer (1988)
lg $\dot{M}$ $[M_\odot yr^{-1}]$	-6.99	Leitherer (1988)

2. Observations and data reduction

Our data sample of HD199478 consists of 41 high-resolution Hα spectra obtained between August 1997 and March 1999 with the coudé spectrograph of the 2 m RCC telescope at the National Astronomical Observatory (Bulgaria). The spectra were collected within an on-going program to study the nature and origin of wind variability in luminous early type stars. The project was started in the spring of 1997 with an ISTA CCD (580x520, 24μ pixel) as a detector. Since October 1998, we have used a PHOTOMETRICS camera equipped with back-illuminated SITe CCD (1024x1024, 24μ pixel). Depending on the configuration used spectra with resolution (R = $\lambda/\delta\lambda$) of 15000 and 22000 were obtained. The spectrum coverage ranges from about 60 to about 200Å. Signal to noise ratio, S/N, of 100 to 300 per pixel in the continuum was usually achieved. The distribution of the observations in time is given in Table 2. In this table Column (2) gives the Julian date of observation; Column (3) records the spectral resolution, R=$\lambda/\delta\lambda$; Column (4) lists the observational window, $\Delta\lambda$ and Column (5) gives the S/N ratio.

The spectra were uniformly reduced using a series of modules written in IDL by one of us (T.V). The procedure is entirely standard and consists of background subtraction, cosmic ray hits removal, flat-fielding and wavelength calibration. Pixel-to-pixel sensitivity variation is taken into account by dividing the spectra by a mean flat-field, obtained as an average during the relevant night. During the wavelength calibration, the correction for the Earth's motion with respect to the heliocentric rest frame is taken into account. The spectra were normalised by a polynomial fit to the continuum, specified by carefully selected spectral windows free of lines.

The atmospheric water vapour lines were removed by dividing each spectrum of HD199478 with a specially constructed "telluric spectrum". This procedure consists of the following steps. First, we observed a rapidly rotating non-variable B star as a telluric standard in the relevant wavelength domains. Second, using an interactive spline-interpolationg technique we obtained a smooth template of the underlying stellar spectrum and subsequently divided the observed spectrum with this template to derive the "telluric spectrum". This was then scaled in order to obtain the best fit for water vapour line profiles on each of the HD199478 spectra, after which the target spectrum was divided with the derived "telluric spectrum" to remove the water vapour lines. Finally, the spectra were rebinned to a step of 0.2Å per pixel.

3. Data analysis

3.1. Hα line-profile variations

That the morphology of the Hα line of HD199478 is temporily variable becomes clear from a simple qualitative comparison of profiles arising from "snapshot" observations separated by months or years. For example, Rosendhal (1973) observed a double-peaked emission with a central absorption at +68km/s while Denizman & Hack (1988) detected profiles consisting of single blue-shifted emission and a weak absorption superimposed on the red emission wing at about +60km s^{-1}.

Table 2. Journal of observations

Date	HJD 2450000+	R	$\Delta\lambda$ (Å)	S/N
1997/08/13	674.314	15000	115	255
1997/08/24	685.448	15000	115	221
1997/09/13	704.519	15000	115	207
1998/03/07	879.509	15000	114	90
1998/05/19	953.410	15000	114	133
1998/06/03	968.430	15000	114	270
1998/06/05	969.566	15000	115	168
1998/06/06	971.453	15000	114	139
1998/06/08	972.581	15000	114	281
1998/06/11	975.600	22000	57	207
1998/06/17	981.581	15000	114	151
1998/06/18	982.579	15000	114	184
1998/07/03	998.291	15000	114	103
1998/07/06	1001.324	15000	114	102
1998/07/07	1002.319	15000	114	120
1998/07/08	1003.432	15000	114	73
1998/07/09	1004.356	15000	114	166
1998/07/11	1006.267	15000	114	179
1998/07/13	1007.584	15000	114	229
1998/07/14	1008.571	22000	58	144
1998/07/15	1009.578	22000	58	200
1998/10/09	1096.306	15000	204	253
1998/11/02	1120.347	22000	102	204
1998/12/30	1178.169	15000	120	112
1998/12/31	1179.169	15000	204	190
1999/01/02	1181.173	22000	102	169
1999/01/06	1185.159	15000	204	135
1999/01/07	1186.171	15000	204	178
1999/01/10	1189.163	15000	204	158
1999/01/26	1205.225	15000	204	85
1999/01/27	1205.669	15000	204	107
1999/02/07	1217.182	15000	204	101
1999/02/08	1217.686	15000	204	159
1999/02/09	1219.187	15000	204	148
1999/03/03	1240.652	15000	204	131
1999/03/04	1241.631	15000	204	137
1999/03/10	1247.553	15000	204	265

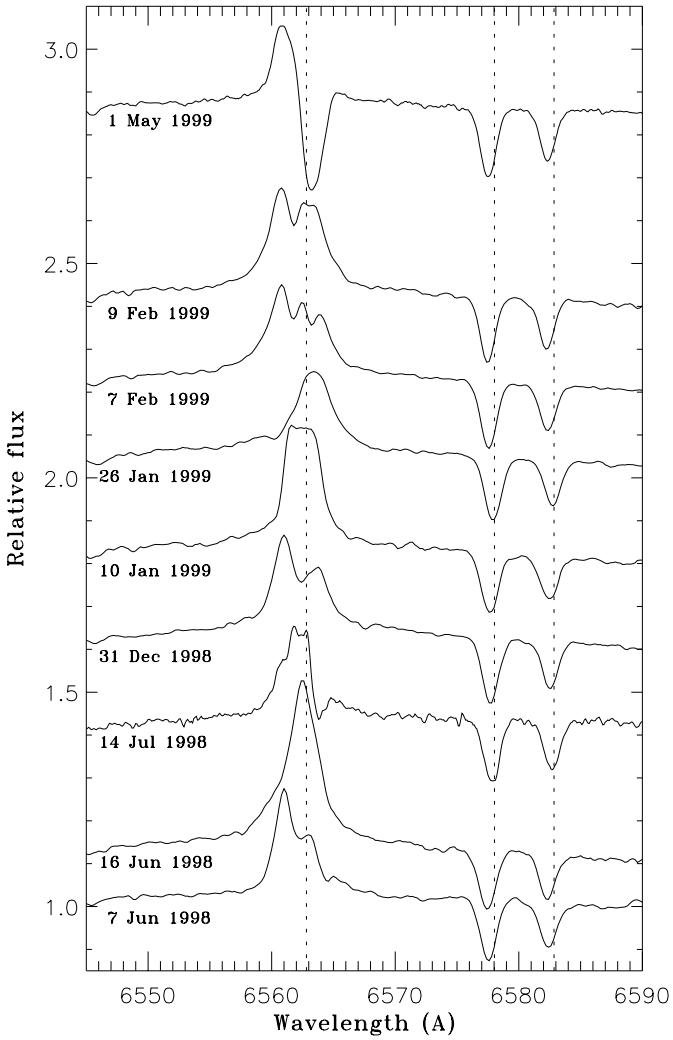

Fig. 1. Examples of differently shaped $H\alpha$ profiles of HD199478 obtained during our observations. On the right of $H\alpha$ the profiles of the CII resonance doublet are seen. Vertical lines represent the laboratory position of each of the three lines.

During our observations a large variety of Hα profile shapes were seen: emission which was almost symmetric and unshifted, with respect to the stellar rest frame; blue- or red-shifted asymmetric emission; double-peaked emission with different values of the V/R intensity ratio; triple-peaked emission and even a reverse P Cygni-type profile. In addition to the well-developed emission core, broad emission wings, extending to more than $\pm$1000 km s^{-1} from the line center, are clearly discernible. Examples of representative $H\alpha$ profiles are displayed in Fig. 1. The spectra are shifted vertically by an amount that ensures better visibility. Two features on the right of Hα belong to the CII resonance doublet. Vertical lines represent the laboratory position of the lines.

To localise the $H\alpha$ variability in an objective and statistically rigorous manner, a simplified version, first reported by Prinja et al. (1996), of the so-called "Time Variance Spectrum" (TVS) analysis (Fullerton et al. 1996) was used. The method consists of a simple computation of the rms deviations, with respect to the mean for a given time-series line profile, as a function of wavelength, σ_λ, under the additional assumption that the noise is dominated by photon noise and is nearly the same for each spectrum in the time series. The quantity σ_λ was calculated using the following expression

$$\sigma_\lambda^2 = \sum_{i=1}^{N} [f_i(\lambda) - F(\lambda)]^2 / [(N-1)F(\lambda)] \quad (1)$$

where $f_i(\lambda)$ is the normalised intensity in the ith of N spectra, and F(λ) is the mean spectrum. In our case N=41. The averaged $H\alpha$ profile and the corresponding TVS are displayed in Fig. 2 as a function of velocity. The rms deviations averaged within the continuum windows is indicated by a dashed line. Statistical significance for variability is represented by a dotted line at a confidence level of 99% probability. Deviations above this level

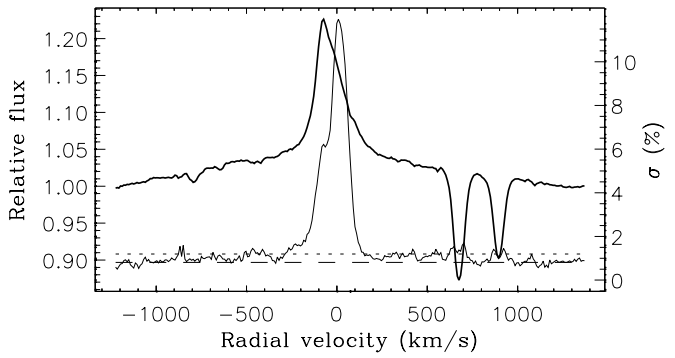

Fig. 2. The averaged $H\alpha$ profile and the rms deviations, σ_λ, for the entire data set as a function of velocity across the line. The threshold for variability (p = 1%) is indicated by a dotted line. The dashed line represents the level of the deviations in the continuum.

must be regarded as genuine variability. Fig. 2 indicates that the region of significant variability is concentrated within the line center and the blue extension of the profile, i.e. between -280 and +150 km s^{-1}. No significant variability in the emission wings of the line is indicated. The fact that the averaged $H\alpha$ profile is blue-shifted and single-peaked, although on several dates during the runs we have detected well-developed double-peaked emission, is certainly due to an observational sampling effect.

The $H\alpha$ spectra obtained during the June-July 1998 and January-February 1999 observations are presented in Fig. 3 in the form of two-dimensional grey scale images ("dynamical spectra"). The spectra are rebinned to velocities within an interval of 48Å with the zero point set at the laboratory wavelength of the line. The intensities are converted into levels of grey according to the scales shown at the right-hand side of the top panels. Gaps between observations if equal or larger than 0.5 days are represented in black. Panels on the top show all spectra plotted within an appropriate intensity interval to display clearly the fluctuation at a specific velocity. The image portions of Fig. 3 indicate that the $H\alpha$ variability manifests itself by variations in position and intensity of emission peak(s). It appears that twice in 1998 and once in 1999 similar patterns of variations were recorded implying that some recurrent phenomenon is likely at work. The recurrent appearance of well-resolved, almost undisplaced absorption, with respect to the systemic velocity, that fades away without changing its position makes an impression. Note also the sudden appearance of weak red-shifted absorption in the second run of the 1998 campaign. The last persists for at least a few days at almost the same velocity, of about +50km s^{-1}, and seems to be similar to that observed earlier by Rosendhal (1973) and Denizman & Hack (1988). The observations do not give evidence for propagating blue-shifted absorption components similar to DACs observed in the UV (Bates & Gilheany 1990).

Since the $H\alpha$ dynamical spectra provided clear evidence for periodic variability, we performed a period analysis, based on the Discrete Fourier Transform and the iterative CLEAN algorithm originally developed by Roberts et al. (1987) in FORTRAN and subsequently reproduced by one of us (T.V) in IDL, for each wavelength bin in the 1998 and 1999 $H\alpha$ series. The obtained results are shown in Fig. 4. The image portions of the figure display a gray-scale representation of the power at a given frequency as a function of position in the line. For the 1998 dataset (left panels of Fig. 4) the periodogram exhibits maximum power at a frequency of 0.0361 day^{-1}, which is concentrated at the center and red extension of the profile. This frequency is equivalent to a period of 27.70 days. The second highest peak is at 0.018 day^{-1} (i.e. 55.5 days), which is longer than the observing period (42 days) and therefore unreliable. The other peaks are probably not significant. For the 1999 dataset (right panel of Fig. 4) the period analysis revealed the presence of periodic variation with a frequency of 0.026 day^{-1}, i.e. 38 days, which is concentrated at the center and blue extension of the $H\alpha$ profile.

To ascertain which of the line parameters is responsible for the periodic variations, detected through Fourier analysis, we measured the velocity of the emission peak(s) and the total equivalent width (EW) of the line. The obtained data are partially shown in Figs. 5 and 6 as a function of JD. Fig. 5 displays variations in velocity of the blue- and red-shifted emission peaks of $H\alpha$ over the June-July 1998 (upper panel) and January-February 1999 (lower panel) observations. The velocity of each feature was measured by bisecting the upper half of its profile. The measurements are corrected for the systemic velocity. The dashed and the solid lines shown in Fig. 5 represent sine curves:

$$V_r = a + bsin\left[\frac{2\pi}{P}(t - t_0)\right] \quad (2)$$

with period P taken from the corresponding Fourier analysis and a, b and t_0 chosen (i.e. not fitted) such that the functions overlays the relevant data reasonably well. The intention of these curves is to guide the eye and to emphasise the periodicity detected by the Fourier analysis. The use of two sine curves (with the same period but of different scaling) is required by the fact that we have two sets of datapoints for each time-series: one for the blue and the other for the red emission peak of the line. The obtained results indicate that: (i) the variations are not symmetric with respect to the line center; (ii) within each observational series the variations in velocity are consistent with the periodicity detected by the corresponding Fourier analysis, i.e. 27.7 days for the 1998 time-series and 38 days for the 1999 time-series. The pattern of variability can be described in the following qualitative way: blue-shifted, asymmetric, single-peaked emission slowly evolves into a double-peaked emission, which in turns evolves into unshifted, almost symmetric single-peaked emission, which changes into asymmetric red-shifted single-peaked emission, which evolves into double-peaked emission and later into blue-shifted, asymmetric, single-peaked emission. We emphasize that the last two phases are not well documented by observations and must therefore be considered as suggestive.

The equivalent width of $H\alpha$ was estimated through line-flux integrating between 6556 and 6568Å. Following the analysis of Chalabaev & Maillard (1983) we estimated the internal precision of individual EW measurements by means of the formula:

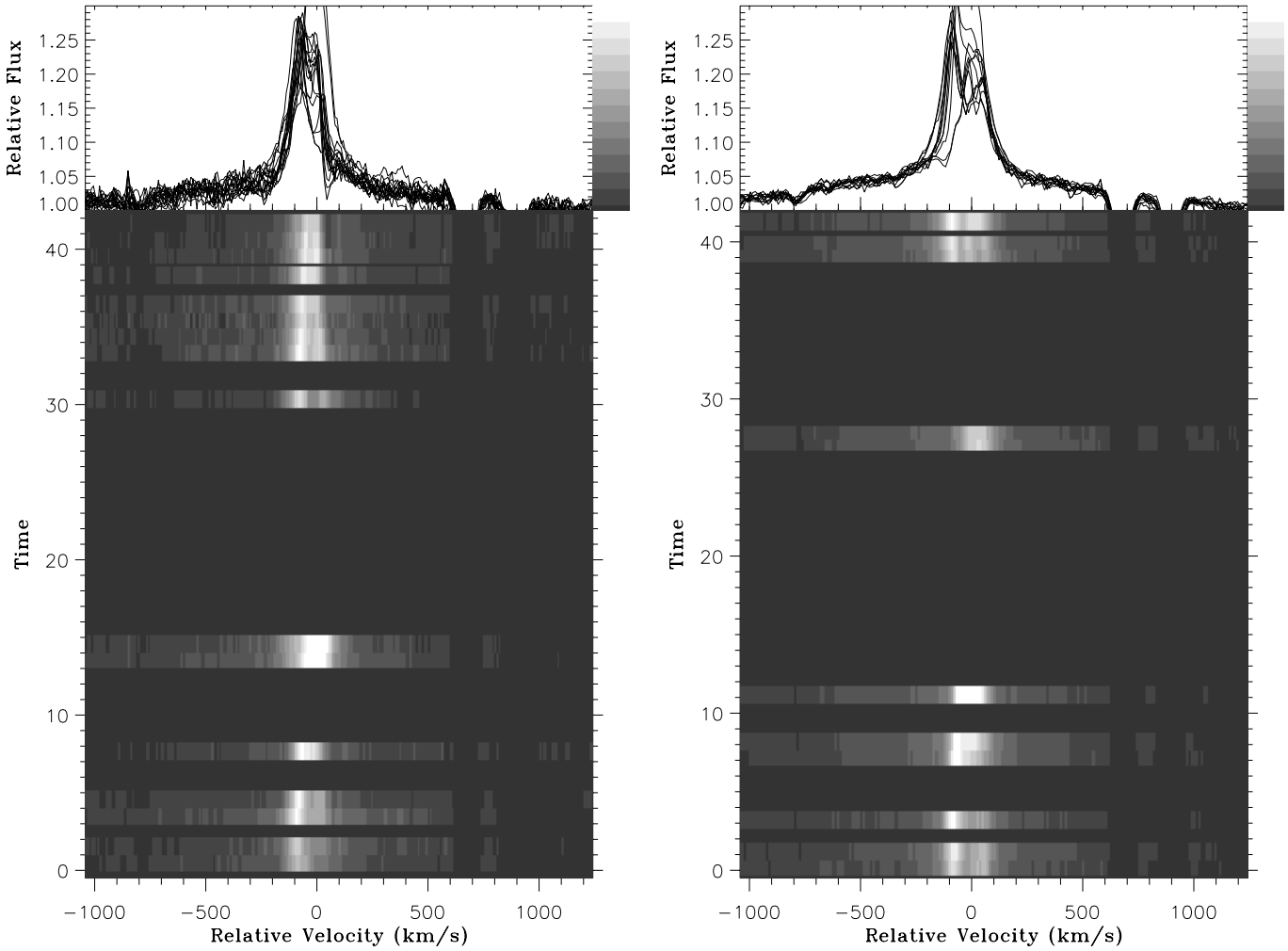

Fig. 3. Dynamical spectra of $H\alpha$ in June-July 1998 (left image) and January-February 1999 (right image). The top panels show an overplot of all profiles from the relevant time series. Time is measured in days. The grey-scale bar on the right of the top panels displays the intensity scaling.

$$\sigma^2(W_\lambda) \;=\; (d_\lambda)^2 \left[\sum_{j=1}^{M} \frac{\sigma(F_j)}{F_c}\right]^2 + \left[\frac{\sigma(F_c)}{F_c}(\Delta\lambda - W_\lambda)\right]^2 \quad (3)$$

where d_λ is the dispersion per pixel, M is the number of pixels including in the wavelength interval $\Delta\lambda$ within which the integration has been done, W_λ is the measured equivalent width. The first term in this equation represents the contribution of the photometric uncertainty to the error, while the second represents the cumulative effect of the uncertainty in the continuum placement over the extent of the profile. In our case the latter effect turned out to be much stronger than the former, due to the large breadth of the $H\alpha$ wings, thus dominating the internal uncertainty of the EW determinations, which in turn was estimated to be always smaller than 10%.

The measurements indicate that the EW of $H\alpha$ varies within 50% of its mean value of -1.24± 0.37Å, obtained as an overall data average. The variations must be genuine since their amplitude exceeds the uncertainty of the individual determinations. There appears to be no clear correlation between variations in EW and changes in position of the emission peaks of $H\alpha$. Fourier analysis performed for the entire dataset did not give evidence for periodic variations in EW. However, an analysis of the data obtained during the 1998 observational campaign showed that the pattern of variability detected is consistent with a periodic variation with P=55.5 days (i.e. a period corresponding to the second highest peak in the relevant periodogram (see Fig. 4, left panel)). This finding is illustrated in Fig. 6 where the solid line represents a sine curve (scaled in an appropriate way) with P=55.5 days. This result implies that the $H\alpha$ emissivity may still vary in some regular way but on a time-scale that is either close to or larger than the length of the observing window and thus is difficult to detect.

Summarising, we conclude that the $H\alpha$ variability in HD199478 is expressed by strong variations in the shape of the profile due to cyclic variation in velocity and intensity of emission peaks accompanied by (cyclic?) variations in total equivalent width of the line. The time-scale of velocity variability is not constant with time. In particular, it equals 27.7 and 38 days

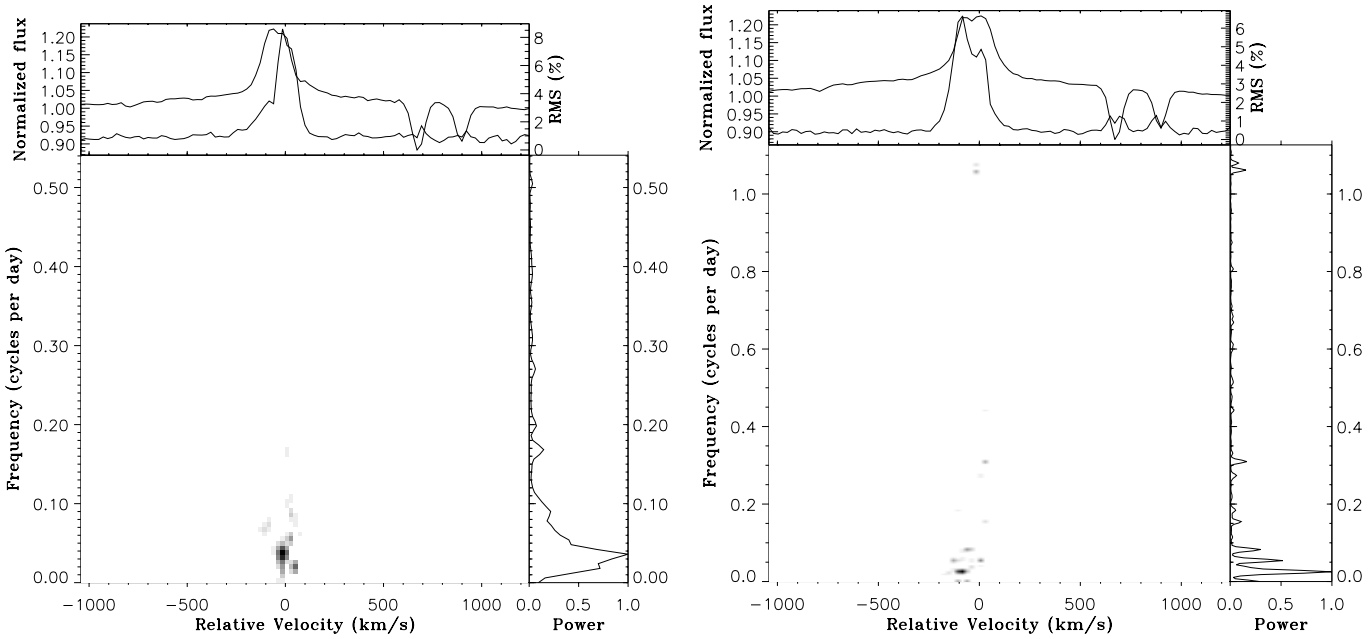

Fig. 4. Temporal variance spectrum and 2d-Fourier transform created from the $H\alpha$ time-series in 1998 (left panels) and 1999 (right panels) The top panels show the average profile and the corresponding TVS. The middle panels display the power at a given frequency as a function of velocity (image portion) and the power summed over the line (right-hand panels).

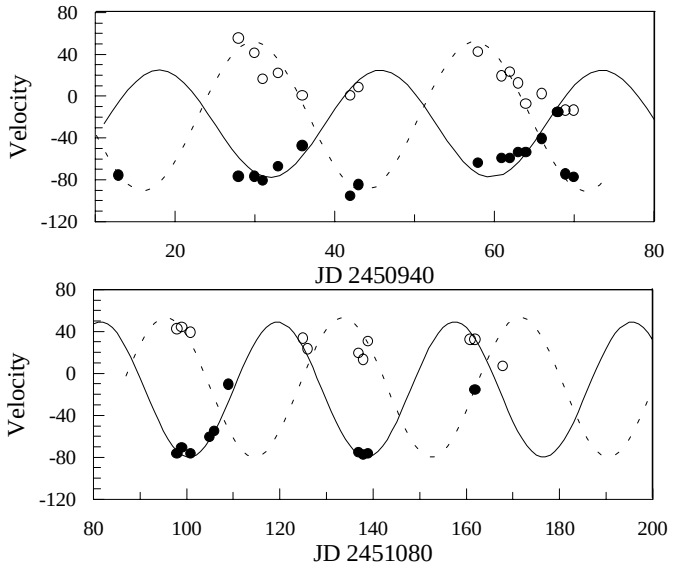

Fig. 5. Variations in velocity of blue- and red-shifted emission peaks of $H\alpha$ as a function of JD for the 1998 (upper panel) and 1999 (lower panel) observations. The measurements are corrected for the systemic velocity. The velocity of blue- and red-shifted emission peaks is represented by dots and open circles, respectively. Sine curves with periods, derived by Fourier analysis, are plotted as a dashed and a solid line to indicate the periodic behaviour in velocity of the two emission peaks. The measurements from the first observational series are consistent with a period of 27.7 days while those from the second series – 38 days.

for the 1998 and 1999 observations, respectively. It is not clear at present what the pattern of EW variability is and whether this

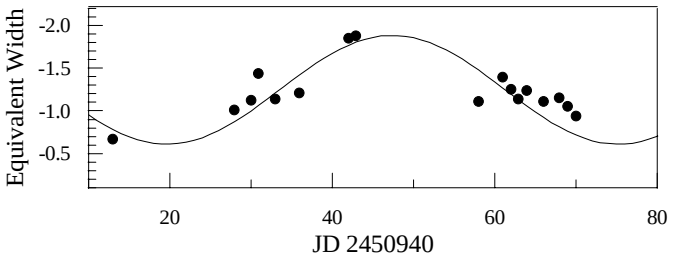

Fig. 6. Variations in EW of $H\alpha$ as a function of JD for the 1998 observational campaigns. **A** sine curve with a period of 55.5 days, derived by the corresponding Fourier analysis, **is** plotted as a solid line to guide the eye and to emphasise the periodicity detected.

variability is related to cyclic variations in the shape of the profile or not. Additional observations on a much longer time-scale are needed to resolve this problem adequately.

3.2. Behaviour of the $HeI\lambda6678$ line and the CII resonance doublet

To gain more information about the depth structure of the transition zone between the photosphere and the wind of HD199478 we examined the lpv of a number of absorption lines situated in the vicinity of $H\alpha$, such as $CII\lambda6578$, $CII\lambda6583$ and $HeI\lambda6678$.

In contrast to Rosendhal (1973), we were always able to detect the CII resonance lines as weak, relatively narrow ($FWHM \sim 70$ km s^{-1}) absorption features superimposed on the red emission wing of $H\alpha$ (between 600 and 1000 km s^{-1}). The averaged CII profiles and the TVS for the entire dataset

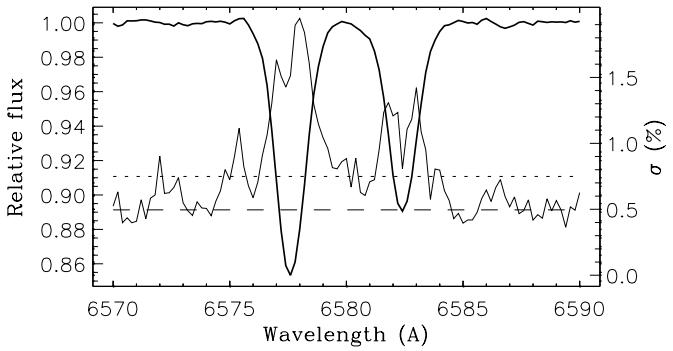

Fig. 7. The averaged profiles of the $CII\lambda6578$ and $\lambda6583$ lines and the TVS spectrum for the entire dataset as a function of wavelength. The level of variability in the continuum and the threshold for significant variability (p = 1%) are indicated by a dashed and a dotted lines, respectively.

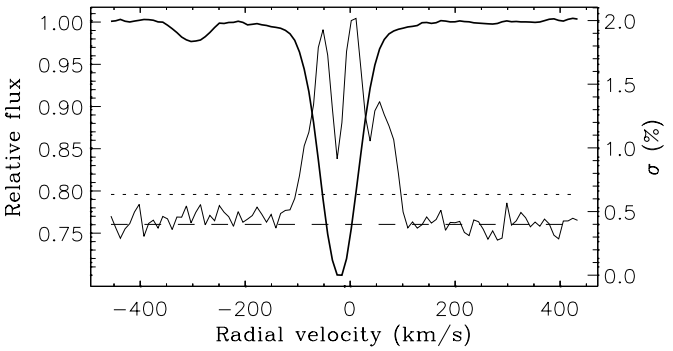

Fig. 8. The averaged $HeI\lambda6678$ profile and the rms deviations, σ_λ, for a subset of 13 spectra, as a function of velocity. The mean level of the deviations in the adjacent continuum is indicated by a dashed line. The dotted line represents the threshold for variability (p = 1%).

are shown in Fig. 7 as a function of wavelength. The level of variability in the continuum is indicated by a dashed line. The dotted line represents the threshold for variability (p = 1%). The shape of the TVS appears to be double-peaked, suggesting existence of radial velocity variability for these lines (Fullerton et al. 1996). The velocity width over which significant variability occurs, ΔV, is equal to 120 and 90 km s^{-1} for the $CII\lambda6578$ and $CII\lambda6583$ lines, respectively.

The measurements show that the lpv detected manifests itself by variations in velocity and line-strength, i.e. EW. In particular, we found that the EW, determined by means of line-flux integration within the profiles, varies within $\pm$13% around a mean value of 0.22 (for $CII\lambda6578$) and 0.16Å (for $CII\lambda6583$). The variations must be genuine since their standard deviations exceed the accuracy of individual determinations (0.01Å), calculated by means of Eq. 3. To determine the velocity of the lines, we fitted a parabola to the lower half of their profiles and used the minimum of the fit as a measure of line position. The mean velocity, derived as an overall data average (N=41), equals -20.6$\pm$4.1 km s^{-1}) and -21.2$\pm$4.5 km s^{-1} for $CII\lambda6578$ and $\lambda6583$, respectively. The rms deviations are larger than the internal uncertainty of our velocity determinations (1.6 km s^{-1}), specified by the rms deviation in velocity of the IS band at λ 6613, thus indicating significant variability in velocity of the CII resonance lines, in agreement with the result derived from the analysis of the TVS. The 2d Fourier analysis performed for the 1998 and the 1999 spectroscopic series did not detect any periodicity for the $CII\lambda6578$ and $CII\lambda6583$ lines. It may well be, however, that this is a result of observational selection. For example, cyclic variations on a time-scale close to or larger than the length of the observing window are difficult to detect.

In the part of our $H\alpha$ spectra (N=13) covering a wavelength range of 204Å, the line $HeI\lambda6678$ is observed as a relatively strong, narrow ($FWHM \sim$ 80 km s^{-1}) symmetric absorption. The averaged $HeI\lambda6678$ profile and the TVS spectrum are displayed in Fig. 8 as a function of velocity. The rms deviations averaged within the adjacent continuum is indicated by a dashed line. The dotted line represents the threshold for variability (p = 1%). The distribution of σ_λ reveals the presence of significant variability concentrated between -100 and +90km s^{-1} (ΔV =190km s^{-1}) within the profile, i.e symmetric about the systemic velocity.

The measurements, performed as described above, showed that the velocity and the strength (i.e. EW) of the line are both variable: the former varies within $\pm$25% around a mean value of - 21.3 km s^{-1} while the latter deviates within $\pm$7% around a mean value of 0.618Å. The variations must be real since their amplitudes exceed the uncertainty in the relevant determinations, which is equal to 10% in velocity and to 2% in EW. Due to the limiting number of available data no time-series analysis was performed for this line.

It is worth noting in addition that the absorption lines of our sample show almost the same values of radial velocity, which are furthermore equal (within the error) to the systemic velocity of -16 km s^{-1} (Denizman & Hack 1988). This finding confirms the photospheric origin expected for these lines. However, the breadth of the lines (i.e. the $FWHM$) is larger than that of a photospheric line with no other broadening than stellar rotation (i.e. V_{rot}sin$i$=45 km s^{-1}). This result indicates that one or more mechanisms exist that additionally broadens the lines. Recent studies, using both LTE and non-LTE techniques (Smartt et al. 1997; Gies & Lambert 1992), have shown that microturbulences of 15 to 30 km s^{-1} appear to be required for B-type supergiants. Thus, we conclude that the line-width excess is likely due (at least partially) to microturbulence in the stellar photosphere.

Summarising, we conclude that absorption lpv consisting of continuous radial-velocity and line-strength (i.e. EW) variations certainly occurs in the spectrum of HD199478. The properties of the studied lines (e.g. radial-velocity and $FWHM$) and the parameters of their TVS (e.g. ΔV) indicate that this variability is more likely coupled to processes in the stellar photosphere. The phenomenon could not be completely interpreted in terms of possible redistribution of a fixed amount of line absorption, as would occur if, e.g., the variability was caused by a macroscopic velocity field alone. Because variations in absorption EW do occur, the process or processes responsible for absorption lpv must also alter the number of absorbers, e.g.

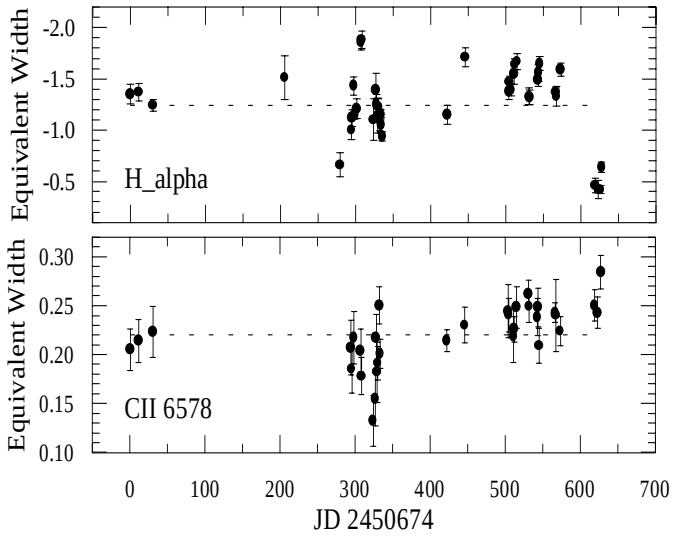

Fig. 9. Variations in the $H\alpha$ equivalent width compared to similar variations in $CII\lambda6582$. The two sets of data show a tendency to anticorrelate.

through changes in the ionization/excitation in the deepest layers of the atmosphere. All this indicates that absorption lpv in HD199478 is more likely caused by variations in velocity and temperature structures of the stellar photosphere.

The presence of significant absorption lpv in HD199478 implies that the variability of $H\alpha$ observed might not be due solely to variations in the physical properties of the wind but also might reflect changes in the underlying photospheric component. To test this possibility, we compared the behaviour of $H\alpha$ (in terms of EW variations) with that of the $CII\lambda6582$ photospheric line. The result, illustrated in Fig. 9, shows that the two sets of data tend to anti-correlate such that an increase in the CII photospheric absorption appears to be accompanied by a decrease in the $H\alpha$ emission. This finding suggests that the $H\alpha$ variability could at least partially be assigned to variations in the underlying photospheric profile.

4. Discussion and conclusions

For the first time an extended data set of high-quality $H\alpha$ spectra with high resolution in wavelength and time was recorded for HD199478. The spectra are analysed in terms of line-profile variability using contemporary techniques of time-series analysis, such as Temporal Variance Spectrum and the 2d-Discrete Fourier Transform. We found that the $H\alpha$ profile of the star consists of a highly variable emission core superimposed on almost constant emission wings. The wings are weak (about 4 to 5% above the continuum) and spread to velocities much higher than the terminal velocity of the wind. The presence of such wings appears to be a common characteristic of the $H\alpha$ profiles of most BA-type supergiants (Kaufer et al. 1996) and is likely due to electron-scattering in the deep atmospheric layers (Hubeny & Leitherer 1989).

Fourier analysis of the two longest time series shows that the $H\alpha$ profile is periodically variable. The periodic component consists of variations in velocity and intensity of blue– and red–shifted emission peaks of the line, which result in drastic alterations in the shape of the profile from almost symmetric and unshifted emission, with respect to the stellar rest frame, through blue- or red-shifted asymmetric emission to double-peaked emission or a reverse P Cygni-type profile. Significant variations in total emissivity (i.e. EW) of the line are also established but these variations do not seem to be obviously linked to changes in the shape of the profile. The source of variability is not clear at present. On the one hand, the TVS of the line clearly indicates that the variations are linked to processes in the wind: the velocity range over which significant variations occur, ΔV=430 km s^{-1}, is larger than $2V_{rot}\sin i$=90 km s^{-1}. On the other hand, the detection of continuous absorption lpv together with the result that the $H\alpha$ emissivity tends to anticorrelate with variations in the strength (i.e. EW) of the $CII\lambda6582$ photospheric line suggest that the $H\alpha$ variability might be assigned (at least partially) to changes in the stellar photosphere. Summarising, we conclude that the $H\alpha$ variability of HD199478 is more likely a result of an interplay between variable wind emission superimposed on variable photospheric absorption.

Absorption line-profile variability consisting of variations in velocity of HI, HeI and metal lines (such as $MgII$, $SiII$ and $FeII$) of HD199478 was first established by Denizman & Hack (1988) through a study of 12 photographic spectra obtained in 1970 and 1986. Our analysis confirmed the presence of continuous radial-velocity variability (typical dispersion of σ=5 km s^{-1}) in photospheric lines and furthermore revealed the existence of significant line-strength (i.e. EW) variations (up to 13% of the mean) for these lines too. The simultaneous appearance of radial-velocity and line-strength variations implies that the variability observed is likely connected to changes in velocity and temperature structures of the stellar photosphere. Unfortunately, the present data do not enable us to perform a detailed study of the phenomenon and to specify its main properties. The relationship (if any) between photospheric line-profile variability and wind variability (traced by $H\alpha$), is also unknown. Long-term, time-resolved, large spectral window observations are needed to adequately resolve the problem of photospheric line-profile variability of HD199478.

Although our data are insufficient to provide deep insight into the nature of the variability of HD199478, some knowledge about the properties of the wind can still be obtained. For example, close inspection of differently shaped $H\alpha$ profiles shows that the envelope of this late-type B supergiant is likely axially-symmetric and disturbed. Indeed, it is obvious that neither blue-shifted emission nor red-shifted absorption can originate from density variations in a spherically symmetric uniformly-distributed stellar wind. On the other hand, double-peaked emission with cyclic V/R variations can be readily interpreted in terms of axial symmetry, e.g. perturbed stellar disks, similar to those in Be stars (Okazaki 1996). However, the appearance of blue-/red-shifted and unshifted single-peaked emission as well as a reverse P Cygni-type profile implies that the phenomenon detected in HD199478 does not appear to be identical to that observed in Be stars. The time-scales of the two are also

quite different – about 4 to 5 weeks for HD199478 and of the order of years and decades for Be stars, making it less likely they are caused by the same mechanism. Thus we conclude that the wind of HD199478 is more likely *axially-symmetric* and *perturbed*, and that the source of wind variability is different from that operating in Be-stars winds. It is worth noting in addition that the detection of blue-shifted absorption components in the UV wavelengths (Bates, Halliwell, Brown-Kerr 1986) also indicates the presence of large-scale structures in the wind of this late-B type supergiant. It is therefore interesting to ascertain if the structures responsible for variations in $H\alpha$ are in some way related to those producing DACs in UV lines, as has been found previously for O-stars winds (Kaper et al. 1997).

Some knowledge of the origin of $H\alpha$ variability could be obtained by analysing the time-scales of the phenomenon observed. For example, the periods derived by Fourier analysis are found to be a factor of twenty longer than the radial flow time of the wind, t_{flow} (t_{flow}(HD199478) = 1.68 days). This result suggests that the variations are not intrinsic to the wind. From the fact that similar patterns of line-profile variability were recorded twice over observations separated by about 5 months (about $90t_{flow}$), one can furthermore suggest that the variations are not transient feature of the wind, but persist for many flow times and must be therefore maintained by photospheric processes. There is some evidence to suggest in addition that the wind of HD199478 might be *rotationally modulated*. On the one hand, the periods of $H\alpha$ variability determined by Fourier analysis are a factor of 3 to 5 longer than the radial fundamental pulsation period $P_{rad,fund}$ =7.8 days. (The later was computed for a pulsation constant log Q = -1.4 used by Kaufer et al. (1996) for BA-type supergiants.) On the other hand, these periods fall just between the rotational periods as estimated from the break-up velocity V_{break}=167.6 km s^{-1} and $v\sin i$, i.e. between 25 and 88 days. These findings imply that rotational modulation could be a possible source of variation in the lower region of the wind, where the $H\alpha$-line forms.

Absorption line-profile variability consisting of radial-velocity and EW variations as well as $H\alpha$ profiles with V/R variations have been observed by Kaufer et al. (1996, 1997) in a sample of 3 late-type B and 3 early-type A supergiants. The former was interpreted as due to pulsation (both radial and non-radial) in the stellar photospheres while the latter was attributed to rotation. A comparison of our results with those published by Kaufer et al. shows that the variability of HD199478 is in many aspects similar to that established in BA-type supergiants, suggesting that the same mechanism is likely responsible for the phenomena observed.

Recent theoretical computations (Pamyatnykh 1998) have predicted a significant extension of the high-order g-mode instability, which causes the variability of Slowly Pulsating B-stars (SPBs) and $\beta Cephei$ stars, to higher luminosity. This prediction was supported by $Hipparcos$ observations, that revealed 72 newly discovered SPBs and 4 $\beta Cephei$ stars, whose position in the HR diagram is fully consistent with the theoretically determined instability domains (Waelkens et al. 1998). In addition, these observations revealed 32 new supergiants with α Cyg-type variations, which inhabit a region extending from the instability strip for g-mode oscillations towards variable B-type supergiants and the instability strip for strange-mode oscillations (Kiriakidis et al. 1993) predicted for more massive stars (e.g. $LBVs$). These results strongly suggest that all early type stars are likely pulsationally unstable. Unfortunately, none of the stars studied by Kaufer et al. nor that studied by us has been ever observed systematically in terms of photometric variation. Thus although they all are known to be photometrically variable neither typical timescales nor behaviour pattern of variability are known at present. Simultaneous photometric and spectral observations are needed to convincingly prove the pulsation origin of the photospheric variability of these stars.

The data presented in this study are obviously insufficient and do not enable the nature and the origin of variability of HD199478 to be investigated completely. The consideration given above concerning the structure and geometry of the wind based on the $H\alpha$ profiles does not take into account the impact of the underlying photospheric profile. A detailed modelling of the presented $H\alpha$ profiles, that takes into account the variability of both the stellar photosphere and the wind, is needed to clarify the picture of variability of HD199478. We are beginning a large ground-based observational program (including spectral and photometric observations) designed to determine the properties of the photospheric line-profile variability and to ascertain whether this variability is related to wind variability (traced by $H\alpha$). The performance of simultaneous photometric observations is very important since it may give information on the nature of the processes that governs this variability.

Acknowledgements. I dedicate this paper to the memory of my friend and colleague Tashko Valchev who not only participated in the observations and did an enormous amount of work on the reduction of the data but also developed all program modules used in the present study. I would like to thank the referee Dr. D.R. Gies for a careful reviewing of the manuscript and valuable comments. This work was supported by NSF to Ministry of Education and Sciences trough grant No. F-813/1998.

References

Baade D., 1992, In: Huber U., Jeffery C.S. (eds.) The Atmospheres of early-Type Stars. Springer, Berlin, p. 45
Bates B., Halliwell D.R., Brown-Kerr W., 1986, Irish Astron. Journal Vol. 17, 256
Bates B., Gilheany S., 1990, MNRAS 243, 320
Chalabaev A., Maillard J.P., 1983, A&A 127, 279
Denizman L., Hack M., 1988, A&AS 75, 79
Fullerton A.W., Gies D.R., Bolton C.T., 1996, ApJS 103, 475
Hubey I., Leitherer C., 1989, PASP 101, 114
Kaper L., Henrichs H.F., Fullerton A.W., et al., 1997, A&A 327, 281
Kaufer A., Stahl O., Wolf B., et al., 1996, A&A 305, 887
Kaufer A., Stahl O., Wolf B., et al., 1997, A&A 320, 273
Gies D.R., Lambert D.L., 1992, ApJ 387, 673
Kiriakidis M., Pricke K.J., Glatzer W., 1993, MNRAS 264, 50
Leitherer C., 1988, ApJ 326, 356
Lennon D.J., Dufton P.L., Fitzsmmons A., 1992, A&AS 94, 569

McErlean N.D., Lennon D.J., Dufton P.L., 1999, A&A 349, 553
Markova N., 2000, A&A 2000, A&AS 144, 391
Markova N., Scuderi S., de Groot M., Panagia N., 2000, A&A submitted
Okazaki A.T., 1996, PASJ 48, 905
Pamyatnykh A.A., 1998, In: Bradly P.A., Guzik J.A. (eds.) PASP Conf. Series 135, p. 268
Percy J.R., Coffin B.L., Drukier G.A., Ford R.P., et al., 1988, PASP 100, 1555
Percy J.R., Harlow J., Haynoe K.A.W., Ivans I.I., et al., 1997, PASP 109, 1215
Prinja R.K., Fullerton A.W., Crowther P.A., 1996, A&A 311, 264
Reid A.H.N., Howarth I.D., 1996, A&A 311, 616
Roberts D.H., Lehar J., Dreher J.W., 1987, AJ 93, 986
Rosendhal J.D., 1973, ApJ 186, 909
Smartt S.J., Dufton P.L., Lennon D.J., 1997, A&A 326, 763
Waelkens C., Aerts C., Kestens E., Grenon M., Eyer I., 1998, A&A 330, 215